NASA TECHNICAL MEMORANDUM

NASA TM X-2043

NASA TM X-2043

MECHANICAL PERFORMANCE OF A 2- TO 10-KILOWATT BRAYTON ROTATING UNIT

by Hugh A. Klassen, Charles H. Winzig, Robert C. Evans, and Robert Y. Wong

Lewis Research Center
Cleveland, Ohio 44135

NATIONAL AERONAUTICS AND SPACE ADMINISTRATION • WASHINGTON, D. C. • JULY 1970

1. Report No. NASA TM X-2043	2. Government Accession No.	3. Recipient's Catalog No.
4. Title and Subtitle MECHANICAL PERFORMANCE OF A 2- TO 10-KILOWATT BRAYTON ROTATING UNIT		5. Report Date July 1970 6. Performing Organization Code
7. Author(s) Hugh A. Klassen, Charles H. Winzig, Robert C. Evans, and Robert Y. Wong		8. Performing Organization Report No. E-5456
9. Performing Organization Name and Address Lewis Research Center National Aeronautics and Space Administration Cleveland, Ohio 44135		10. Work Unit No. 120-27 11. Contract or Grant No. 13. Type of Report and Period Covered
12. Sponsoring Agency Name and Address National Aeronautics and Space Administration Washington, D.C. 20546		Technical Memorandum 14. Sponsoring Agency Code
15. Supplementary Notes		

16. Abstract

An accumulated total test time of 1005 hr was compiled at various temperature, pressure, and power levels with argon, krypton, and the design mixture of helium and xenon. The performance of the gas-lubricated bearings is presented, including component motions, bearing loads, observations of pneumatic hammer, hydrostatic flow rates, thrust bearing clearances, transient performance, and bearing ambient pressure. Predicted internal temperatures are compared with actual temperatures for three power levels.

17. Key Words (Suggested by Author(s))	18. Distribution Statement
Brayton rotating unit Pivoted pad gas bearing Internal temperature control Pneumatic hammer	Unclassified - unlimited

19. Security Classif. (of this report)	20. Security Classif. (of this page)	21. No. of Pages	22. Price*
Unclassified	Unclassified	27	$3.00

*For sale by the Clearinghouse for Federal Scientific and Technical Information
Springfield, Virginia 22151

MECHANICAL PERFORMANCE OF A 2- TO 10-KILOWATT BRAYTON ROTATING UNIT

by Hugh A. Klassen, Charles H. Winzig, Robert C. Evans, and Robert Y. Wong

Lewis Research Center

SUMMARY

A single-shaft turbine-compressor-alternator package for a Brayton Cycle power generation system was tested at the NASA Lewis Research Center. The rotor operates on gas-lubricated bearings. The testing included 1005 hours of hot operation and covered a wide range of pressure, temperature, and power levels. Bearing operation was stable at all times. There was no appreciable change in the size or nature of any of the bearing component motions. Shaft orbit diameters were approximately 0.0001 inch (0.00025 cm). The motions of the gimbal and thrust runner were influenced by temperature and pressure level. None of the bearing component motions exceeded 0.002 inch (0.0005 cm). Clearance between the thrust runner and thrust stator was smaller on the compressor side than on the turbine side. The clearance on the compressor side varied between 0.0004 and 0.0005 inch (0.0010 and 0.0013 cm) and decreased with increasing turbine inlet temperature and decreasing system pressure level. Journal bearing loads, as indicated by film pressure measurements, remained relatively constant at about 15 pounds (6.8 kg). During hydrostatic operation, pneumatic hammer occurred in the turbine journal bearing when the ratio between supply pressure and bearing ambient pressure exceeded values of 10. Hammering was not allowed to occur during normal operation. It was prevented by maintaining bearing pressure ratios below the threshold value of 10. Shaft orbits showed large increases in the critical speed ranges. The largest orbit diameter obtained was 0.00085 inch (0.0022 cm) at 8100 rpm. The Brayton rotating unit (BRU) rotor has been accelerated and decelerated through the critical speed range approximately 90 times without incident. With the bearings externally pressurized, the shaft was allowed to rotate backwards at speeds up to 600 rpm and then suddenly accelerate in the forward direction. The initial backward rotation did not appear to influence bearing performance. The compressor bleed flow used to pressurize the bearing housing was 1.2 percent of total compressor flow. There was generally good agreement between predicted and actual Brayton rotating unit internal temperatures. Alternator winding temperatures were somewhat higher than predicted.

INTRODUCTION

The NASA Lewis Research Center is investigating the potential of the Brayton cycle for electrical power generation systems in space. One phase of this investigation involves ground testing components designed for Brayton cycle space power plants. One of these components is a single-shaft turbine-compressor-alternator package. The rotor operates on gas-lubricated journal and thrust bearings. The package was procured under a contract with the AiResearch Manufacturing Co. of Arizona and has been designated the Brayton rotating unit (BRU). The BRU is described in reference 1.

Reliable operation of the BRU requires reliable bearing operation and safe temperatures within the machine. The bearings must be designed for stable operation over a wide range of ambient pressure levels, turbine inlet temperatures, rotative speeds, rotative acceleration rates, and power levels. In addition, the moving parts must not be subject to rapid wear or fatigue. Since turbine inlet temperatures vary from ambient to 2060° R (1144 K), package temperatures must be controlled to maintain proper clearances and bearing loads, to protect low-temperature components such as alternator windings, and to limit thermal stresses.

The BRU was installed in a test loop in order to evaluate its performance. The test loop was designed so that the BRU could be operated over a wide range of turbine and compressor inlet temperatures, pressure levels, and power outputs, including the design values. This test loop is described in reference 1.

This report presents results obtained during 1005 hours of operation in the test loop under a wide variety of operating conditions. Turbine inlet temperatures were varied from 1460° to 2060° R (811 to 1144 K), and power output was varied from 1.0 to 15 kilowatts. Three working fluids were used: argon, krypton, and the design mixture of helium and xenon with a molecular weight of 83.8. During most of the time, the turbine inlet temperature was close to the design value of 2060° R (1144 K).

The following information is presented:

(1) Bearing operating characteristics, which include component motions, bearing loads, pneumatic hammer, hydrostatic bearing flow rates, transient behavior, and thrust clearances

(2) Operating characteristics of the bearing housing pressurization system

(3) A comparison of actual temperatures throughout the BRU with predicted temperatures for three power levels

BRAYTON ROTATING UNIT DESIGN CONDITIONS

Turbomachinery

The 10.7-kilowatt design operating conditions for the BRU turbomachinery are as follows:

Working fluid	Helium-xenon mixture
Working fluid molecular weight	83.8
Mass flow rate, lb/sec (kg/sec)	
Turbine	1.33 (0.604)
Compressor	1.35 (0.612)
Turbine	
Inlet temperature, ^{o}R (K)	2060 (1144)
Inlet pressure, psia (N/cm^2 abs)	45.9 (31.6)
Total- to static-pressure ratio	1.75
Compressor	
Inlet temperature, ^{o}R (K)	540 (300)
Inlet total pressure, psia (N/cm^2 abs)	24.2 (16.7)
Total pressure ratio	1.9
Shaft speed, rpm	36 000

The difference in turbine and compressor flow results from the fact that approximately 2 percent of compressor flow is bled into the bearing housing to maintain bearing ambient pressure.

Alternator

The 10.7-kilowatt design operating conditions for the alternator are as follows:

Power, kW	10.7
Power factor	0.85
Frequency, Hz	1200
Liquid coolant flow, lb/sec (kg/sec)	0.12 (0.054)

Gas Bearings

The 10.7-kilowatt design operating conditions for the gas bearings are as follows:

Lubricant	Helium-xenon mixture
Bearing pad temperature, ^{o}R (K)	845 (469)
Ambient pressure, psia (N/cm^2 abs)	43.9 (30.3)

BRAYTON ROTATING UNIT DESCRIPTION

A schematic drawing of the BRU is shown in figure 1(a). The radial-inflow turbine rotor and the centrifugal compressor impeller are mounted on the ends of the shaft with the alternator between. The two journal bearings are located on either side of the alternator. The thrust bearing is between the compressor impeller and the compressor end journal bearing.

Bearings

Both the journal and thrust bearings are designed for self-acting operation at design speed. The bearings must be externally pressurized during low-speed operation, including startup and shutdown. During the testing described in this report, external pressurization (jacking gas) was supplied at speeds below 30 000 rpm.

Journal bearings. - Each journal bearing has three pivoted pads. The pads and pivots are shown in figure 2. The pivot location is 65 percent of the pad length from the leading edge. The pads are made of M-41 tool steel with a Rockwell C hardness of 60 to 65. The pivot consists of a fully conforming sliding contact ball and socket, both made of tungsten carbide. External pressurization is supplied through a hole in the pivot center to a single orifice in each pad. The balls of two of the pivots in each bearing are rigidly mounted to the frame. The third ball is mounted on a flexible beam. The purpose of this flexible beam is to accommodate small amounts of differential growth that tend to change bearing clearances and loads. The growth can result from thermal or centrifugal forces. Changes in load were minimized by selecting a low spring rate with a nominal value of 2000 pounds per inch (357 kg/cm). During assembly, the flexible beam is deflected to establish an initial bearing load (preload), and the shaft is thus clamped between the three bearing pads. The preload is required because of the low spring rate. The preload value is selected to provide the desired bearing load during operation. Bearing ambient pressure is maintained by a bleed from the compressor discharge. The turbine and compressor labyrinth seals (fig. 1(a)) are sized to limit this bleed to 2 percent of the compressor flow. Ambient pressure control is required to maintain adequate bearing film thicknesses.

Thrust bearing. - The double-acting thrust bearing is shown in figure 3. The bearing consists of a flat thrust runner and two stator plates, each with nine self-acting stepped sectors. Each sector is provided with an orifice in the land for external pressurization during startup and shutdown. The thrust stator material is M-50 tool steel with a Rockwell C hardness of 62 to 64. The entire thrust bearing is mounted on a gimbal assembly for self-alinement purposes.

Brayton Rotating Unit Internal Temperature Control

Various methods are used to limit the BRU internal temperatures. The design features of the temperature control system are shown in figure 1(b) and are as follows:

(1) A portion of the back of the turbine scroll is gold plated. The gold low-emissivity surface reduces radiant heat transfer from the turbine.

(2) The turbine seal holder is rhodium plated to maximize reflection of radiant heat.

(3) A portion of the rotor at the turbine end has a low cross-sectional area to minimize conduction heat flow from the turbine. There is another area of low cross section between the turbine scroll and its mounting flange.

(4) The turbine end curvic coupling provides high resistance to conduction heat flow.

(5) A copper heat shunt carries heat around the turbine bearings to be removed by the alternator coolant system.

(6) Two copper heat shunts inside the shaft are designed to prevent thermal distortion by eliminating temperature gradients at the bearings.

(7) The alternator coolant system removes heat due to alternator electrical losses and heat conducted through the rotor.

(8) The compressor impeller serves as a heat sink.

(9) Seal leakage flow removes about 30 percent of the heat that is conducted from the turbine wheel toward the curvic coupling.

APPARATUS

The closed-loop test facility is described in detail in reference 1. It was designed for operation at turbine inlet temperatures up to the design value of 2060° R (1144 K). The maximum turbine inlet pressure is approximately 45 psia (31 N/cm^2 abs), corresponding to a power output of approximately 13.5 kilowatts at design turbine and compressor inlet pressure.

The heat source consists of direct resistance electrical heaters in the turbine inlet line. The cooler is a gas-to-liquid heat exchanger capable of cooling the turbine exit gas to 460° R (256 K). Auxiliary systems include alternator cooling, voltage and speed control, simulated vehicle load, inventory control, and jacking gas. Startup is accomplished either by injecting gas into the heater inlet, thus creating a pressure ratio across the turbine, or by operating the alternator as a motor.

INSTRUMENTATION

Chromel-Alumel thermocouples were used to measure temperatures. Strain-gage transducers were used to measure pressures. The compressor weight flow was measured with a Venturi flowmeter in the inlet line. The compressor bleed flow was measured with a rotameter. Loop data were recorded by high-speed automatic data recorders and processed through a digital computer.

Motions of the shaft and bearing were measured with noncontact capacitance probes. These probes were included in the BRU design. Four probes were used for shaft orbit motions. At each journal bearing, the shaft orbit was determined by two probes 90^{o} apart in a radial plane. Four probes were used to measure thrust plate motion and thrust film thickness. Three probes measured the film thickness on the turbine side, and the fourth measured film thickness on the compressor side. Eight probes measured the motions of the leading edges of journal bearing pads. Two probes measured the motions of the corners of one of the turbine solidly mounted pads. Two probes measured the motions of the corners of the turbine flexibly mounted pads. The compressor bearing pad instrumentation was identical to that of the turbine. Two probes measured thrust bearing gimbal motions. Compressor and turbine bearing loads and radial motions of the flexibly mounted pads were each determined by a probe that measured the motions of the beam-type springs. Sixteen of the capacitance probe outputs were monitored on dual-beam oscilloscopes. All probe outputs were continuously recorded on an FM magnetic tape recorder.

Speed was measured in the following ways:

(1) Two capacitance probes produced signals with frequencies proportional to rotative speed. Six recesses on the shaft circumference produced varying clearances between the probes and the shaft.

(2) Alternator output frequency was measured with a counter.

Loop data were recorded by high-speed automatic data recorders and were processed through a digital computer. During starts, 50 data points were recorded at a rate of 2500 points per second. These included temperatures, pressures, thrust bearing film thicknesses, and electrical data. For steady-state operation, 200 data points were recorded at a rate of 20 points per second.

PROCEDURE

The BRU was operated with three working fluids. For the first 250 hours of hot testing, the working fluid was krypton, which has the same molecular weight as the design helium-xenon mixture. Because of a leak to the atmosphere, argon, which is relatively inexpensive, was used for the second 275 hours. In both cases, the turbine inlet

temperature was approximately 2000° R (1100 K), and the turbine inlet pressure was approximately 25.5 psia (17.6 N/cm^2 abs). Power outputs were approximately 6 kilowatts for krypton and 4.6 kilowatts for argon.

During the remaining 480 hours of hot testing, the working fluid was the design helium-xenon mixture with a molecular weight of 83.8. The operating characteristics of the BRU were examined over a range of conditions. The turbine inlet temperature was varied from 1460° to 2060° R (811 to 1144 K), the power level was varied from 1.0 to 15 kilowatts, and the compressor inlet temperature was varied from 510° to 580° R (284 to 322 K).

RESULTS AND DISCUSSION

Part of the BRU performance evaluation consisted of accumulating 1005 hours of operation at essentially steady-state conditions. During most of this time, the turbine inlet temperature was close to the design value of 2060° R (1144 K). Three working fluids were used: argon, krypton, and the design helium-xenon mixture with a molecular weight of 83.8. During helium-xenon operation, the turbine inlet temperature was varied from 1460° to 2060° R (811 and 1144 K), and the power level was varied from 2.3 to 15 kilowatts.

This report covers the mechanical performance of the BRU. The results are presented in three sections: (1) gas bearing performance, (2) bearing housing ambient pressure, and (3) internal temperature distribution.

Bearing Performance

Bearing component motions. - Bearing operation was stable throughout the test with no deterioration in performance. Photographs of the bearing oscilloscope traces were taken throughout the 1005 hour test. These photographs show no measurable change with time in the peak-to-peak values or in the shapes of the traces.

The bearing traces are shown in figure 4. These photographs were taken at 990 hours at a turbine inlet temperature of 2060° R (1144 K) and a turbine inlet pressure of 45 psia (31 N/cm^2 abs), corresponding to a power output of 13.5 kilowatts. Each small division on the grid represents 0.0001 inch (0.00025 cm), except for the thrust bearing traces, where one division represents approximately 0.000087 inch (0.00022 cm).

The compressor end journal orbit is shown in figure 4(a), and the corresponding time traces are shown in figure 4(b). The orbit is slightly elliptical with a major axis of 0.0001 inch (0.00025 cm).

The turbine end journal orbit is shown in figure 4(c) and the corresponding time traces in figure 4(d). The orbit is roughly circular with a diameter of 0.00011 inch (0.00028 cm).

The two top traces of figure 4(e) show the motions of the corners of the leading edge of the flexibly mounted pad at the turbine end. The two waves are in phase, showing that the pad has a plain pitching motion. The two bottom traces show the motions of the leading edge of one of the turbine solidly mounted pads at the turbine end. These two waves are also in phase. The travel of the flexibly mounted pad leading edge is 0.00019 inch (0.00048 cm) as compared with 0.00010 inch (0.00025 cm) for the solidly mounted pad. The flexibly mounted pad has the greater motion because the flexible beam allows radial motion of the pivot. The traces of the solidly mounted pad appear to have a double frequency trace superimposed on a shaft frequency trace. This type of motion was encountered during a previous test of a turbocompressor with pivoted pad bearings and is discussed in reference 2.

The top trace in figure 4(f) shows the motion of one corner of the leading edge of the compressor flexibly mounted pad. This trace shows a motion of 0.00015 inch (0.00038 cm) and is similar to the traces for the turbine flexibly mounted pad. The bottom trace is for the compressor fixed mounted pad. The motion is only 0.00005 inch (0.00013 cm).

The radial motions of the flexibly mounted beam and pad assemblies are shown in figure 4(g). The top trace shows the motions at the turbine end. Both have a magnitude of 0.00013 inch (0.00033 cm). The two traces are almost 180° out of phase, indicating that shaft motion is essentially conical.

The motions of the two opposite sides of the thrust runner with respect to the thrust stator are shown in figure 4(h). The two probes used for these traces were in line with each other. The top trace is the turbine side. Both motions are about 0.00008 inch (0.00020 cm). Figure 4(i) shows the motions caused by the thrust bearing gimbal mount. The traces show the motions of the thrust stators with respect to the frame. The two gimbal probes are located on the compressor side of the thrust bearing at the same radial distance from the shaft centerline. The probe axes are perpendicular to the thrust stator faces and are separated by an angle of 90°, measured in a radial plane. The probe for the top trace is in the same axial plane as the thrust bearing probes for figure 4(h). The movements are 0.0001 inch (0.00025 cm) for the top trace and 0.00005 inch (0.00013 cm) for the bottom trace. In both cases, most of the motion is caused by a subsynchronous motion superimposed on the 600-hertz gimbal motions associated with rotative speed. The subsynchronous frequency is approximately one-fifth to one-sixth of the shaft frequency.

The bearing component motions were independent of the working fluid. In general, these motions were also independent of operating conditions. However, when turbine inlet pressure was increased well above the 6-kilowatt design point of 25.8 psia (17.8 N/cm^2 abs), a slight increase in the motion was indicated by the lower gimbal trace.

This increase was due to the subsynchronous motion mentioned in the preceding paragraph. At higher turbine inlet pressures, both gimbal motions increased as the turbine inlet temperature was decreased below the design value of 2060° R (1144 K). In addition, the motions of the thrust runner relative to the thrust stator also increased with decreasing turbine inlet temperature. Figure 5 shows the effect of high turbine inlet pressure and low turbine inlet temperature on the gimbal and thrust motions. Figure 5(a) represents the 6-kilowatt design operation. (A complete set of traces for the 6-kW design condition is shown in ref. 1.) Turbine inlet pressure is 25.8 psia (17.8 N/cm^2 abs), and turbine inlet temperature is 2060° R (1144 K). Figure 5(b) shows the thrust and gimbal motions at turbine inlet conditions of 45 psia (31 N/cm^2 abs) and 1660° R (922 K). Both thrust traces are for the turbine side of the bearing. The bottom trace corresponds to the turbine trace in figure 5(a). At the 6-kilowatt design operation (fig. 5(a)), there is no subsynchronous component in the bottom gimbal trace or in either thrust trace. At the high pressure and low temperature (fig. 5(b)), this component is present in all these traces. None of the motions shown in figure 5(a) exceeds 0.0002 inch (0.0005 cm).

Bearing loads. - Journal bearing loads were computed from the difference between hydrodynamic film pressures measured at the orifice and bearing ambient pressure. Experimental data obtained with argon indicate that bearing load is equal to approximately 0.80 times this pressure difference. The data were obtained using the BRU bearing configuration installed in the simulator version of the machine described in reference 3. A discussion of the correlation between load and bearing pressure differential is given in the appendix. Journal bearing loads were nearly constant for all working fluids and operating conditions. These loads were in the range of 14 to 15 pounds (6.4 to 6.8 kg). The relatively constant bearing loads are an indication that clearance between the bearing shoes and shaft remained almost constant.

Pneumatic hammer. - When jacking gas is applied to the bearings, pneumatic hammer sometimes occurs in the journal bearings. Tests were made at zero speed to determine the conditions at which pneumatic hammer occurs. Jacking gas pressures were varied from 70 to 180 psia (48 to 124 N/cm^2 abs). Pneumatic hammer could be induced over this entire pressure range. At a given jacking gas pressure, pneumatic hammer can be induced by decreasing housing pressure and can be eliminated by increasing housing pressure. The minimum jacking gas-to-housing pressure ratio required to induce pneumatic hammer varied from 10 to 16. Between a pressure ratio of 10 and 16, pneumatic hammer did not always occur spontaneously but could sometimes be started or stopped by striking the BRU with a mallet. Above a pressure ratio of 16, pneumatic hammer always occurred. Below a pressure ratio of 10, pneumatic hammer was never observed. In some cases after the hammer was induced, the BRU shaft was allowed to rotate backward at speeds up to 300 rpm. The hammering continued during rotation, and the oscilloscope traces were unaffected. Pneumatic hammer was not a problem

during the test program because jacking gas-to-housing pressure ratios were kept below the threshold value of 10.

Some of the oscilloscope traces obtained during pneumatic hammer are shown in figure 6. Journal bearing pressure was 149 psia (103 N/cm^2 abs) with a pressure ratio of 16.2 across the bearings. Shaft traces are not shown, since shaft motion was very small compared with bearing pad motion. The top two traces in figure 6(a) show the motion of the corners of the leading edge of the turbine end flexibly mounted pad. The bottom two traces show the corners of the leading edge of one of the turbine end solidly mounted pads. The leading edge movement for the flexibly mounted pad is approximately 0.0006 inch (0.0015 cm). Motion for the solidly mounted pads is about 0.0001 inch (0.0002 cm). The top trace of figure 6(b) shows the motions of one corner of the leading edge of the compressor end flexibly mounted pad. The bottom trace shows the same motion for a compressor end solidly mounted pad. The movement of the flexibly mounted pad is approximately 0.0008 inch (0.00030 cm). The motion of the solidly mounted pad is only about 0.00001 inch (0.000025 cm). Figure 6(c) shows the radial motions of the turbine and compressor end flexibly mounted pivots. Turbine end pivot movement is shown in the top trace. The turbine and compressor end pivots move 0.0006 and 0.0001 inch (0.0015 and 0.00025 cm), respectively.

The frequencies of all traces are approximately 1000 hertz, except for the turbine end solidly mounted pad which shows frequencies of about 2000 hertz. Because of the solid mounting, these traces must represent a pitching motion. The wave form of the traces for the turbine end flexibly mounted pads can be produced by summing two sine waves, one of which has twice the frequency of the other. Since the turbine flexibly mounted pivot has a radial motion with a frequency of 1000 hertz, the leading edges of this pad should also have a component of radial motion with the same frequency. It seems likely that the traces for the turbine flexibly mounted pads are the sum of a 1000-hertz radial motion and a 2000-hertz pitching motion. All the compressor traces are considerably smaller than the corresponding turbine traces. This difference may be caused by the shaft motion originating at the turbine end of the shaft rather than by pneumatic hammer at the compressor end. Figure 7 shows the traces at the same jacking gas pressure with the pressure ratio increased to 22.4. In this case, amplitudes of the turbine end motions changed with time, producing amplitude-modulated waves.

Hydrostatic flow rates. - Design information for jacking gas systems was provided by measuring jacking gas flow rates at zero speed. The supply pressure to all bearings was approximately 150 psia (103 N/cm^2 abs) at a temperature of 540° R (300 K). The total flow to the journal bearings was 1.23×10^{-3} pound per second (5.59×10^{-4} kg/sec). The total flow to the thrust bearings was 6.72×10^{-3} pound per second (3.05×10^{-3} kg/sec).

Thrust bearing clearances. - The clearance between the thrust runner and the compressor thrust stator is always smaller than the clearance on the turbine side of the

bearing. For self-acting operation, these clearances are approximately 0.0004 inch (0.0010 cm) for the compressor side and 0.0021 inch (0.0053 cm) for the turbine side. This difference in clearances shows that the load is always toward the compressor. The thrust bearing load is composed mostly of the rotor weight and the net aerodynamic load of the compressor and turbine. Since the BRU was tested in a vertical position with the compressor down, the rotor weight acts toward the compressor. The thrust loads of the turbine and compressor act in opposite directions, away from the BRU.

Clearance between the thrust runner and the compressor thrust stator is measured by a single capacitance probe. The probe readings did not show a clear correlation between turbine inlet pressure and thrust clearance. The lack of correlation may be due to the dampers that were built into the gimbal system. Damping, which was provided for stability, could cause variations in the alinement between the thrust stator and the thrust runner. The pressure differential between the hydrodynamic film and the bearing housing (bearing ΔP) should provide a more reliable indication of changes in thrust clearance. Film pressure is measured by a pressure transducer in the jacking gas line. During hydrodynamic operation, this measurement provides an average of the film pressure at the nine orifices. This pressure should be affected less by small alinement changes than by the single probe reading. As the turbine inlet pressure was increased at constant temperature, the bearing ΔP decreased. This decrease indicates a decrease in net thrust load and an increase in thrust clearance on the compressor side of the bearing. Since clearance increases with pressure level, the thrust bearing is adequate for any power output which can be obtained. As the turbine inlet temperature was decreased at constant turbine inlet pressure, bearing ΔP and the capacitance probe both indicated an increase in clearance.

Bearing transient performance. - During startup and shutdown, two journal bearing critical speed regions are encountered. In the critical speed regions, large increases occur in the shaft orbits. The orbit sizes depend on the amount of shaft unbalance and on the rate of rotative acceleration. The largest orbits occur during shutdown because of the low rate of deceleration. At 6600 rpm, during shutdown, the turbine and compressor end shaft orbits are 0.0007 and 0.0008 inch (0.0018 and 0.0020 cm), respectively. At 8100 rpm, the increase in the turbine end orbit is small, but the compressor end orbit increases to 0.00085 inch (0.0022 cm). If the shaft is sufficiently well balanced, the critical speed regions are not a hazard. The BRU rotor has been accelerated and decelerated through the critical speed range approximately 90 times without incident.

When jacking gas is applied to the bearings, the shaft rotates backwards because of the bearing design. Since the pivot is closer to the trailing edge than the leading edge, the gas pressure forces the leading edge away from the shaft so that most of the flow is in the direction of the leading edge. The resulting net drag force toward the

leading edge produces the backward rotation of the shaft. This rotation can be prevented by bleeding gas into the turbine or by energizing the alternator field. One possible start mode for other installations is to allow the shaft to rotate backwards before starting. Tests were run to determine if the sudden reversal in direction was a hazard to the bearings. The shaft was allowed to rotate backwards at speeds up to 600 rpm and then was accelerated forward at rates comparable to those occurring in actual starts. The initial backward rotation did not appear to affect bearing performance during acceleration.

Bearing Housing Ambient Pressure

The bearing ambient pressure was maintained by bleeding a portion of the compressor discharge flow into the bearing housing. Part of the bleed flow passes through the compressor labyrinth seal and enters the compressor diffuser inlet. The remainder passes through the turbine seal and enters the turbine rotor inlet (see fig. 1(a)). Because of the low flow through the seals, the bearing housing pressure is essentially equal to the compressor discharge pressure. The measured compressor bleed flow was 1.2±0.1 percent of the compressor flow for all operating conditions. Since the compressor bleed flow lowers the thermodynamic efficiency of the powerplant, it should be kept at the lowest value consistent with safe seal clearances.

Brayton Rotating Unit Internal Temperatures

As part of the BRU design procedure, the contractor prepared thermal maps showing predicted temperatures throughout the package. These maps were essential in setting such design standards as

(1) Materials
(2) Initial clearances and control of clearance changes
(3) Cooling requirements for alternator and bearings
(4) Shunting and removal of waste heat from the remainder of the package
(5) Rotor tie bolt tension
(6) Control of bearing load changes

In table I, predicted temperatures for power levels of 2.25, 6.0, and 10.5 kilowatts at a power factor of 0.85 are compared with measured temperatures at approximately the same electrical outputs. The actual value of power factor was approximately 0.95. The working fluid is helium and xenon, the turbine inlet temperature is 2060^{o} R (1144 K) and the rotative speed is 36 000 rpm. Figure 8 shows the thermocouple locations corresponding to the thermocouple numbers given in the table. In reference 1, predicted and actual temperatures are compared for krypton and argon working fluids.

The BRU internal temperatures generally are in good agreement with the predicted temperatures. The only potentially serious temperature control problem is the alternator armature winding temperatures that are measured by thermocouples 1 to 8. These windings were designed for continuous operation at 428° F (220° C). Table I shows that at 10.5 kilowatts, which is close to the alternator nameplate rating of 10.7 kilowatts, all the temperatures are below this value. The maximum temperature is 403° F (206° C). Figure 9 shows the maximum winding temperature as a function of alternator power output for the design turbine inlet temperature of 2060° R (1144 K). The maximum recommended winding temperature is 428° F (220° C). This temperature is reached at a power output of 11.3 kilowatts. At 15 kilowatts, the winding temperature reaches 495° F (257° C). The alternator windings are the limiting factor in determining the maximum continuous power output. At 10.5 kilowatts, table I shows discrepancies of 92° F (51° C) and 103° F (57° C) between the actual and predicted temperatures for thermocouples 3 and 4, respectively. According to the manufacturer, thermocouples 1 to 8 may be improperly labeled. In this case, the actual discrepancy might only be about 25° F (14° C).

Because the winding temperatures were higher than predicted, alternator coolant flow was increased from the design value of 0.12 pound per second (0.054 kg/sec) to 0.15 pound per second (0.068 kg/sec). This flow increase did not produce an appreciable decrease in winding temperatures. During the 1005-hour test, alternator coolant inlet temperatures varied from approximately 520° to 535° R (289 to 297 K). Since these variations occurred at times when other operating conditions were changing, no general correlation was established between coolant inlet and alternator winding temperatures.

SUMMARY OF RESULTS

This report presented the results of an investigation of the mechanical performance of a single-shaft turbine-compressor-alternator package designed for a Brayton cycle power generation system. The results include the gas bearing operating characteristics, the operation of the bearing housing pressurization system, and the temperature distribution through the package and are summarized as follows:

1. During the 1005-hour test of the Brayton rotating unit (BRU), the oscilloscope traces of the bearing component motions showed no measurable change in the sizes of the motions or in the wave shapes. Bearing operation was stable with no deterioration in bearing performance.

2. Shaft orbit diameters were approximately 0.0001 inch (0.00025 cm). None of the bearing component motions exceeded 0.0002 inch (0.0005 cm).

3. At turbine inlet pressures above 37 psia (25.5 N/cm^2 abs), gimbal and thrust bearing motions increased as the turbine inlet temperature was decreased from the design value of 2060° R (1144 K).

4. Turbine and compressor journal bearing loads were computed from film pressure measurements. These loads remained approximately constant at about 15 pounds (6.8 kg) for all operating conditions.

5. During hydrostatic operation, pneumatic hammer sometimes occurred in the turbine journal bearing. The hammering started when the pressure ratio between the bearing supply and the bearing cavity was increased to a value between 10 and 16. Frequency of the hammer was about 1000 hertz. Hammering did not occur during normal hydrostatic operation because bearing pressure ratios were below the threshold value of 10.

6. Clearance between the thrust runner and the compressor thrust stator was always smaller than the clearance on the turbine side of the thrust bearing. The compressor thrust bearing clearance increased with increasing pressure and with decreasing turbine inlet temperature. The clearances for the test conditions covered in this report varied between 0.0004 and 0.0005 inch (0.0010 and 0.0013 cm).

7. Shaft orbits showed large increases in the critical speed ranges. The largest orbit diameter obtained was 0.00085 inch (0.0022 cm) at 8100 rpm. The BRU rotor has been accelerated and decelerated through the critical speed range approximately 90 times without incident.

8. When jacking gas was applied to the bearings, the shaft rotated backwards. The shaft was allowed to rotate backwards at speeds up to 600 rpm and then was suddenly accelerated in the forward direction. The initial backward rotation did not appear to affect the bearing performance.

9. The compressor bleed flow used to pressurize the bearing housing was 1.2 ± 0.1 percent of the total compressor flow for all operating conditions.

10. In general, there was good agreement between actual and predicted BRU internal temperatures from 2.25 to 10.5 kilowatts. The alternator winding temperatures were somewhat higher than predicted. The maximum recommended winding temperature of 428° F (220° C) was reached at a power output of 11.3 kilowatts with a design turbine inlet temperature of 2060° R (1144 K).

Lewis Research Center,
National Aeronautics and Space Administration,
Cleveland, Ohio, February 24, 1970,
120-27.

APPENDIX - DETERMINATION OF BEARING LOAD FROM BEARING FILM PRESSURE AND AMBIENT PRESSURE

For BRU-type journal bearings, there is an approximate linear relation between bearing load and the bearing ΔP. The bearing ΔP is defined as the difference between the film pressure at the pad orifice and the bearing ambient pressure. Figure 10 shows the variation of load with bearing ΔP. The bearing ambient pressure was 16 psia (11 N/cm^2 abs), and the rotative speed was 36 000 rpm. These data were obtained using the BRU bearing configuration installed in the simulator version of the machine described in reference 3.

The flexibly mounted pads in the simulator are mounted on diaphragms rather than beams. The first step in obtaining data for figure 10 was to determine a zero-speed curve of diaphragm deflection against bearing load. The bearing load was varied by loading the shaft with weights. Diaphragm deflection was measured with capacitance probes. The data of figure 10 were then obtained at 36 000 rpm by measuring bearing ΔP values at various loads. The load was varied by applying differential pressures across the diaphragm. The total bearing load is the algebraic sum of the load corresponding to the capacitance probe reading and the force due to the differential pressure across the diaphragm.

Since figure 10 shows a straight-line relation between load and bearing ΔP, bearing load is the product of bearing ΔP and the slope of the line. A value of 0.8 was used for the slope to compute bearing loads for the BRU tests described in this report.

During self-sustaining operation, BRU journal bearing loads cannot be obtained from capacitance probe readings. Experimental curves of load against beam deflection are only valid when internal temperatures are maintained near room temperature. At actual operating temperatures, the clearance between the flexible beam and the probe is apparently influenced by thermal effects such as expansion and distortion. The indirect method actually used for load determination was necessary because of errors caused by elevated temperatures. Although the data of figure 10 also depend on capacitance probe readings, errors were minimized by operating the simulator at temperatures close to ambient. The simulator is driven by a small drive turbine that operates on cold air rather than with high-temperature working fluid. The turbine and compressor rotors are not enclosed and act as heat sinks to remove heat generated by the bearings. Cooling gas is passed over the bearing pads for additional heat removal.

REFERENCES

1. Wong, Robert Y.; Klassen, Hugh A.; Evans, Robert C.; and Winzig, Charles H.: Preliminary Investigation of a Single-Shaft Brayton Rotating Unit Designed for a 2- to 10-Kilowatt Space Power Generation System. NASA TM X-1869, 1969.

2. Wong, Robert Y.; Klassen, Hugh A.; Evans, Robert C.; and Spackman, Donald J.: Use of an Electronic Visualization Technique in the Study of Gas Journal Bearing Behavior. NASA TM X-1609, 1968.

3. Anon.: Design and Fabrication of a High-Performance Brayton Cycle Radial-Flow Gas Generator. NASA CR-706, 1967.

TABLE I. - COMPARISON OF PREDICTED AND ACTUAL TEMPERATURE

DISTRIBUTION FOR OPERATION WITH HELIUM-XENON MIXTURE

Thermo-couple	Design		Actual		Design		Actual		Design		Actual	
	Turbine inlet pressure, psia (N/cm^2 abs)											
	13.7 (9.45)		14.7 (10.1)		25.8 (17.8)		22.7 (15.7)		43.2 (29.8)		34.4 (23.7)	
	Turbine inlet temperature, ^{o}R (K)											
	2060 (1144)		2034 (1130)		2060 (1144)		2054 (1141)		2060 (1144)		2069 (1149)	
	Compressor inlet pressure, psia (N/cm^2 abs)											
	7.6 (5.24)		8.0 (5.52)		14.2 (9.79)		12.1 (8.34)		23.7 (16.3)		18.3 (12.6)	
	Compressor inlet temperature, ^{o}R (K)											
	540 (300)		534 (297)		540 (300)		534 (297)		540 (300)		535 (297)	
	Power output, kW											
	2.25		3.5		6.0		6.4		10.5		10.5	
	Operating temperature											
	^{o}F	^{o}C	^{o}F	^{o}C	^{o}F	^{o}C	^{o}F	^{o}C	^{o}F	^{o}C	^{o}F	^{o}C
1	225	107	168	76	275	135	196	91	375	191	233	112
2	225	107	189	87	250	121	224	107	375	191	263	128
3	170	77	259	126	200	93	318	159	300	149	392	200
4	170	77	273	134	200	93	335	168	300	149	403	206
5	250	121	262	128	300	149	323	162	400	204	398	203
6	170	77	215	102	200	93	259	126	300	149	317	158
7	170	77	213	101	200	93	257	125	300	149	319	159
8	170	77	214	101	200	93	256	124	300	149	320	160
9	130	54	125	52	140	60	134	57	160	71	143	62
10	130	54	133	56	135	57	133	56	160	71	144	62
11	130	54	135	57	145	63	144	62	175	79	148	64
12	128	53	117	47	135	57	123	51	155	68	127	53
13	380	193	320	160	300	149	329	165	375	191	327	164
14	380	193	327	164	300	149	330	166	375	191	327	164
15	380	193	322	161	300	149	333	167	375	191	333	167
16	185	85	154	68	190	88	163	73	200	93	168	76
17	185	85	157	69	190	88	164	73	200	93	170	77
18	185	85	174	79	190	88	188	87	200	93	201	94
19	170	77	181	83	225	107	188	87	200	93	189	87
20	350	177	359	182	360	132	392	200	440	227	426	219
21	210	99	211	99	230	110	233	112	265	129	255	124
22	185	85	191	88	210	99	220	104	250	121	245	118
23	380	193	386	197	364	184	388	198	385	196	387	197
24	380	193	389	198	364	184	389	198	385	196	392	200
25	(a)	(a)	307	153	(a)	(a)	311	155	(a)	(a)	315	157
26	(a)	(a)	308	153	(a)	(a)	312	156	(a)	(a)	316	158
27	316	158	335	168	326	163	340	171	355	179	339	171
28	316	158	332	167	326	163	339	171	355	179	342	172
29	(a)	(a)	274	134	(a)	(a)	280	138	(a)	(a)	278	137
30	(a)	(a)	284	140	(a)	(a)	286	141	(a)	(a)	284	140
31	380	193	400	204	360	182	393	201	380	193	394	201
32	380	193	399	204	360	182	394	201	380	193	396	202
33	340	171	350	177	360	182	345	174	380	193	342	172
34	750	399	989	532	600	316	958	514	500	260	901	483
35	1025	552	1154	623	1025	552	1169	632	1025	552	1183	639
36	900	482	1065	574	900	482	1079	582	1000	538	1100	593

[a]Not available.

TABLE I. - Concluded. COMPARISON OF PREDICTED AND ACTUAL TEMPERATURE

DISTRIBUTION FOR OPERATION WITH HELIUM-XENON MIXTURE

Thermo-couple	Design		Actual		Design		Actual		Design		Actual	
	Turbine inlet pressure, psia (N/cm^2 abs)											
	13.7 (9.45)		14.7 (10.1)		25.8 (17.8)		22.7 (15.7)		43.2 (29.8)		34.4 (23.7)	
	Turbine inlet temperature, ^oR (K)											
	2060 (1144)		2034 (1130)		2060 (1144)		2054 (1141)		2060 (1144)		2069 (1149)	
	Compressor inlet pressure, psia (N/cm^2 abs)											
	7.6 (5.24)		8.0 (5.52)		14.2 (9.79)		12.1 (8.34)		23.7 (16.3)		18.3 (12.6)	
	Compressor inlet temperature, ^oR (K)											
	540 (300)		534 (297)		540 (300)		534 (297)		540 (300)		535 (297)	
	Power output, kW											
	2.25		3.5		6.0		6.4		10.5		10.5	
	Operating temperature											
	^oF	^oC	^oF	^oC	^oF	^oC	^oF	^oC	^oF	^oC	^oF	^oC
37	200	93	246	119	220	104	263	128	240	116	281	138
39	278	137	286	141	278	137	287	142	278	137	290	143
40	278	137	236	113	278	137	286	141	278	137	288	142
41	278	137	238	114	278	137	238	114	278	137	242	117
42	255	124	276	136	260	127	276	136	260	127	278	137
43	(a)	(a)	87	31	(a)	(a)	83	28	(a)	(a)	83	28
44	240	116	241	116	240	116	249	121	250	121	258	126
45	240	116	253	123	240	116	257	125	250	121	265	129
46	240	116	239	115	240	116	247	119	250	121	253	123
47	200	93	197	92	220	104	206	97	220	104	217	103
48	200	93	201	94	220	104	212	100	220	104	222	106
49	200	93	192	89	220	104	205	96	220	104	216	102
50	220	104	125	52	250	121	125	52	260	127	128	53
51	360	182	163	73	350	177	164	73	350	177	164	73
52	300	149	185	85	300	149	182	83	300	149	188	87
53	300	149	185	85	300	149	189	87	300	149	189	87
54	300	149	119	48	300	149	121	49	300	149	121	49
55	(a)	(a)	98	37	(a)	(a)	98	37	(a)	(a)	100	38
56	(a)	(a)	88	31	(a)	(a)	87	31	(a)	(a)	91	33
57	(a)	(a)	127	53	(a)	(a)	131	55	(a)	(a)	136	58
58	375	191	429	221	300	149	449	232	350	177	463	239
59	375	191	430	221	300	149	440	227	350	177	444	229
60	375	191	428	220	300	149	449	232	350	177	461	238
61	375	191	414	212	300	149	436	224	350	177	451	233
66	700	371	909	487	700	371	944	507	800	427	976	524
67	1000	538	1164	629	1000	538	1190	643	1000	538	1211	655
68	1300	704	1357	736	1400	760	1384	751	1400	760	1406	763
69	1300	704	1339	726	1400	760	1364	740	1400	760	1383	751
70	1300	704	1351	733	1400	760	1380	749	1400	760	1409	765
71	1600	871	1516	824	1600	871	1544	840	1600	871	1569	854
72	1600	871	1510	821	1600	871	1543	839	1600	871	1570	854
73	1600	871	1509	821	1600	871	1543	839	1600	871	1570	854
74	1500	816	1462	794	1525	829	1495	813	1525	829	1523	828
75	1500	816	1456	791	1525	829	1487	808	1525	829	1515	824
76	1500	816	1461	794	1525	829	1492	811	1525	829	1518	826
77	(a)	(a)	1223	622	(a)	(a)	1229	665	(a)	(a)	1233	667
78	(a)	(a)	1172	633	(a)	(a)	1189	643	(a)	(a)	1201	649

[a]Not available.

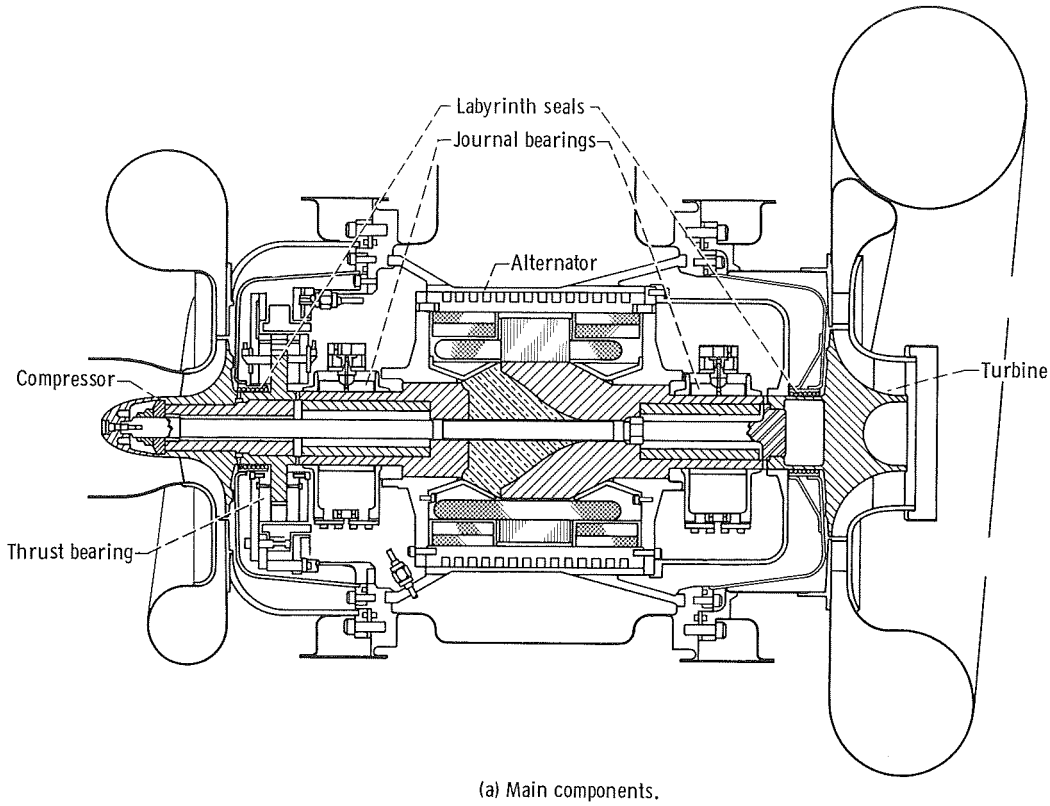

(a) Main components.

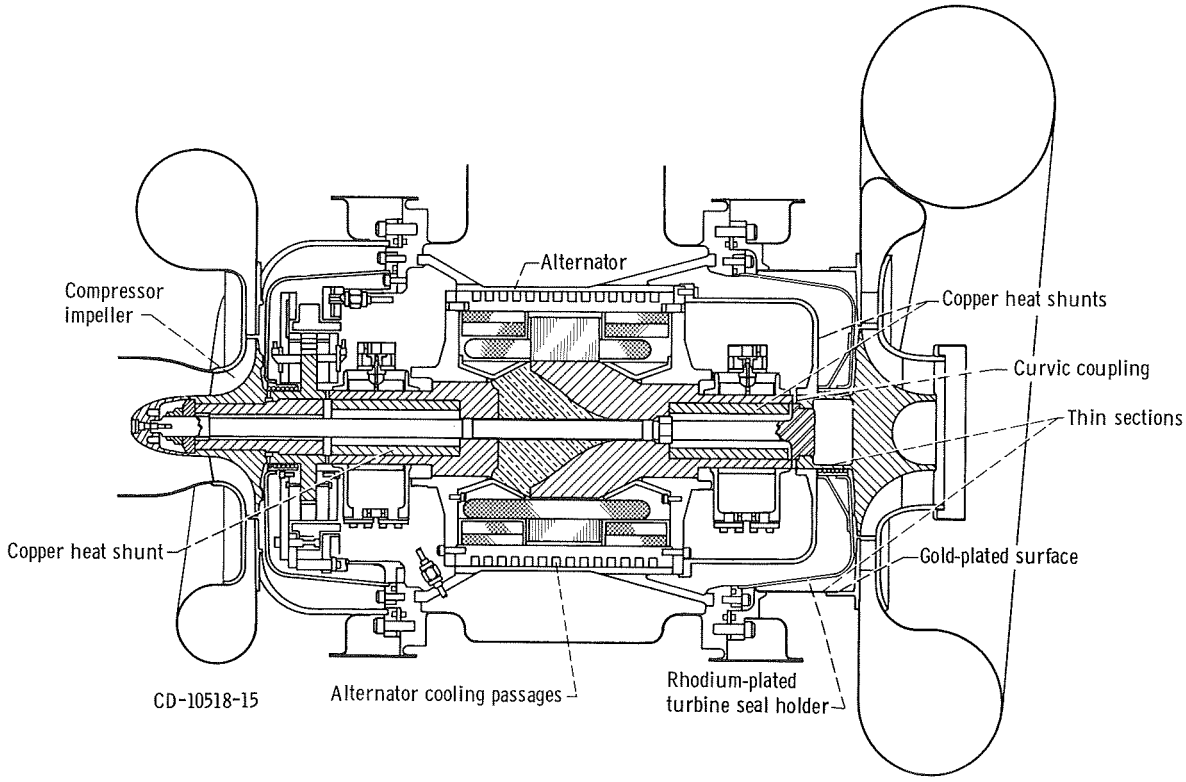

(b) Temperature control system.

Figure 1. - Brayton rotating unit cross section.

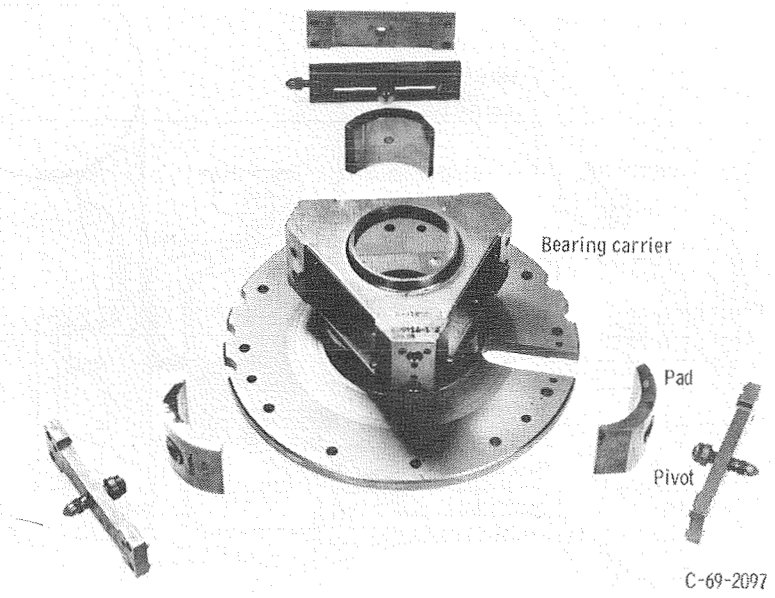

Figure 2. - Journal bearing assembly.

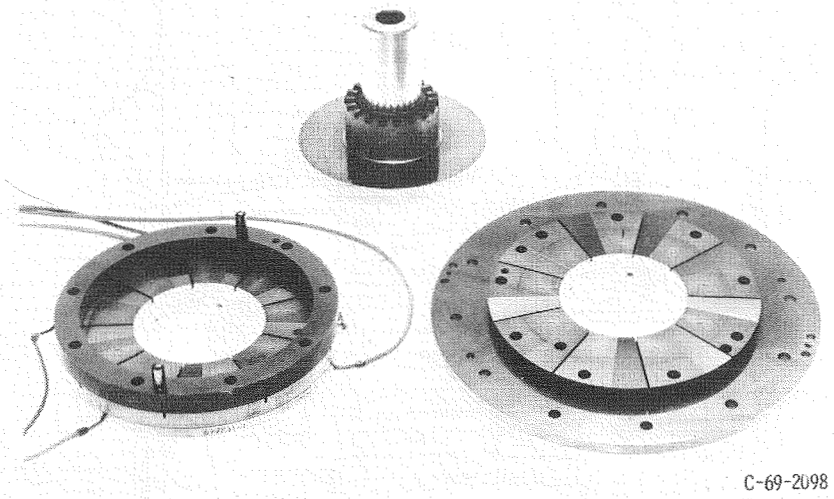

Figure 3. - Thrust bearing stators and runner.

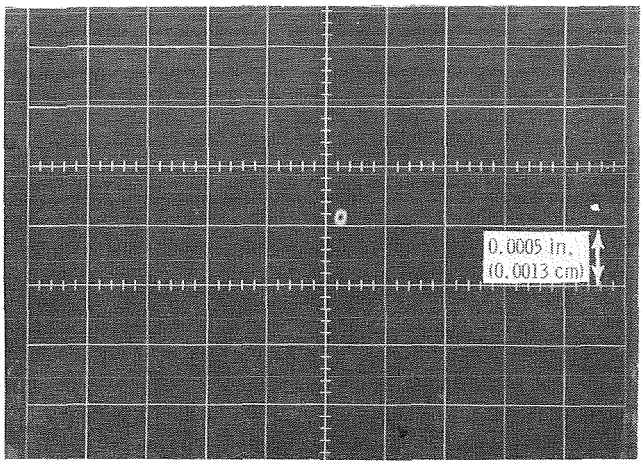

(a) Shaft orbit at compressor journal bearing.

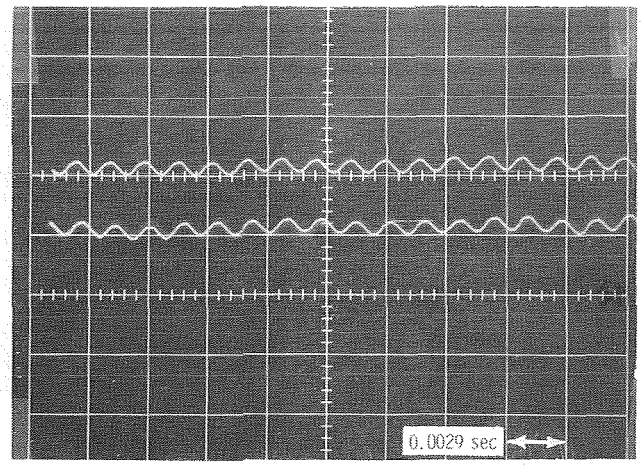

(b) Shaft motions at compressor journal bearing; orthogonal probes.

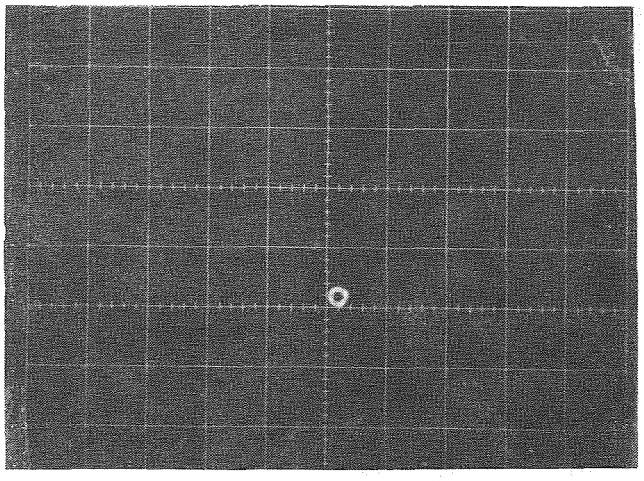

(c) Shaft orbit at turbine journal bearing.

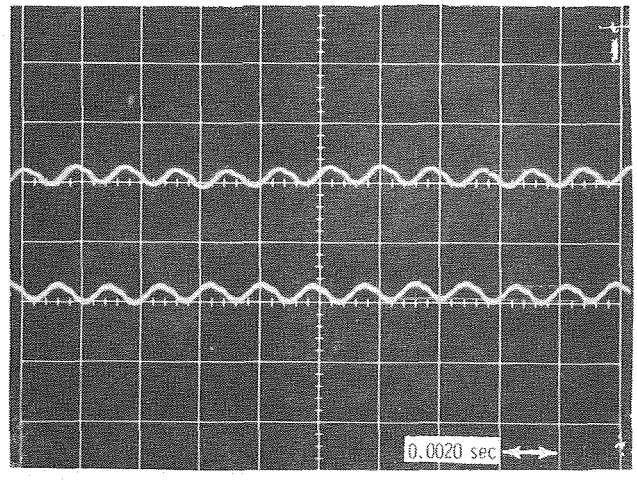

(d) Shaft motions at turbine journal bearing; orthogonal probes.

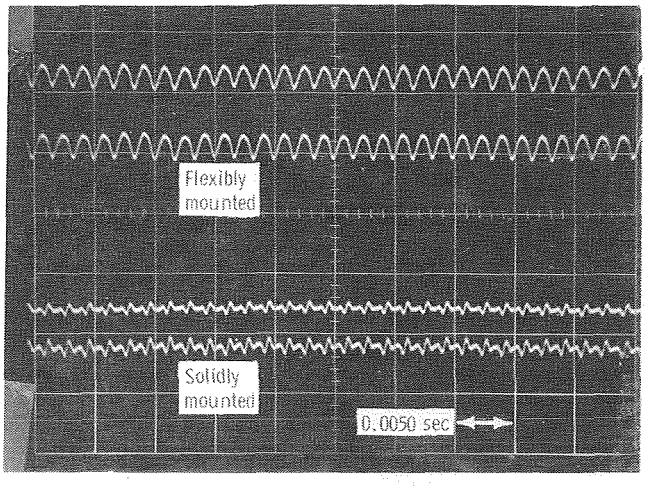

(e) Motions of leading edges of turbine journal bearing pads.

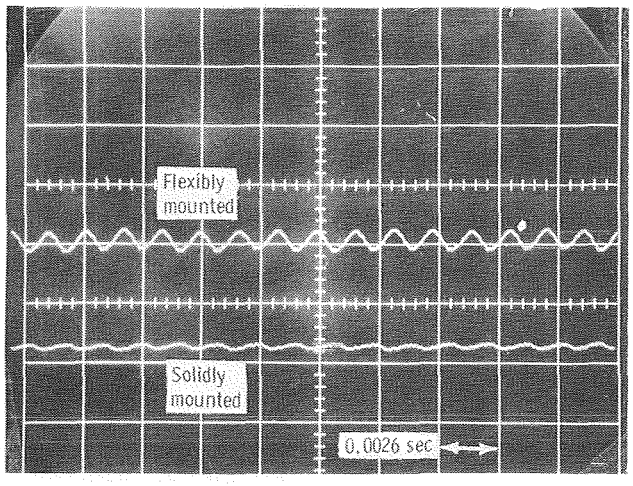

(f) Motions of leading edges of compressor journal bearing pads.

Figure 4. - Oscilloscope traces of bearing component motions.

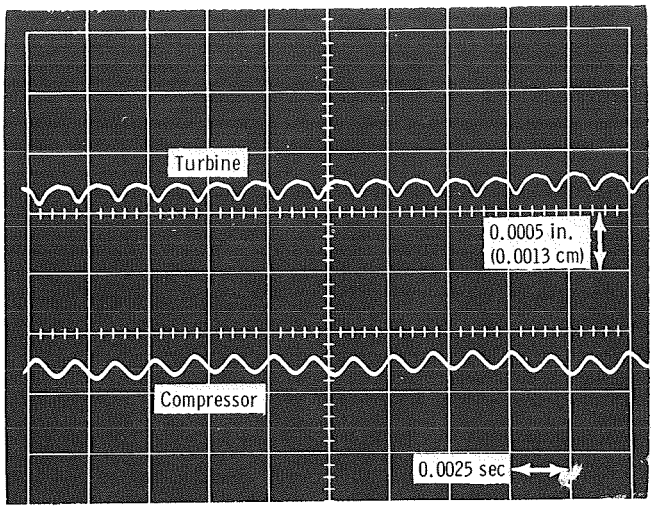

(g) Radial motions of flexibly mounted pads and pivots; turbine and compressor journal bearings.

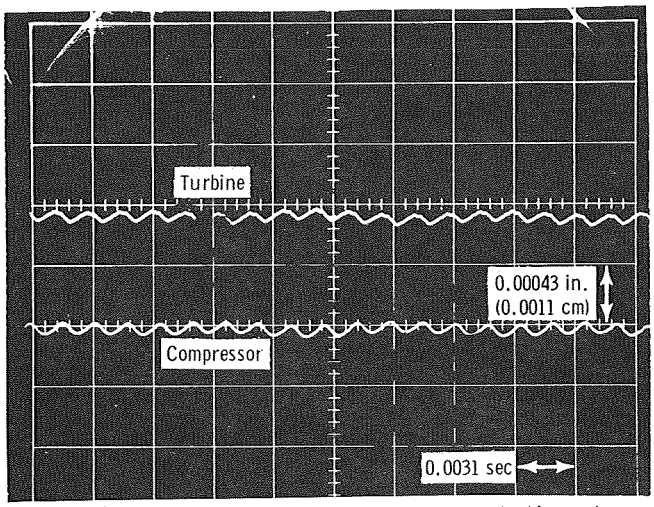

(h) Motions of thrust runner relative to thrust stators on turbine and compressor sides of thrust bearing.

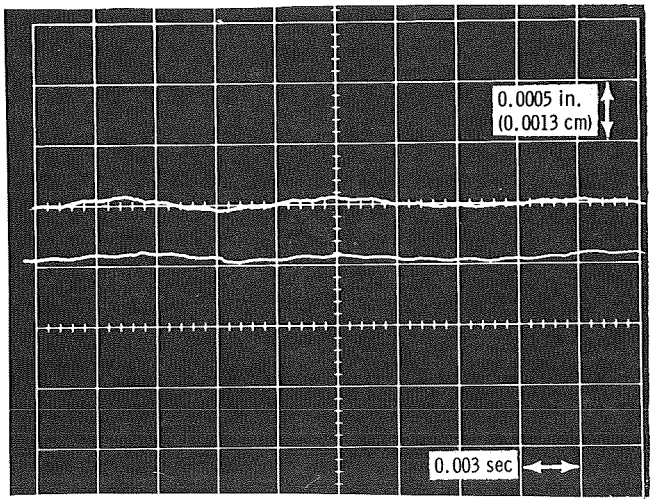

(i) Motions of thrust stator with respect to frame; gimbal traces.

Figure 4. - Concluded.

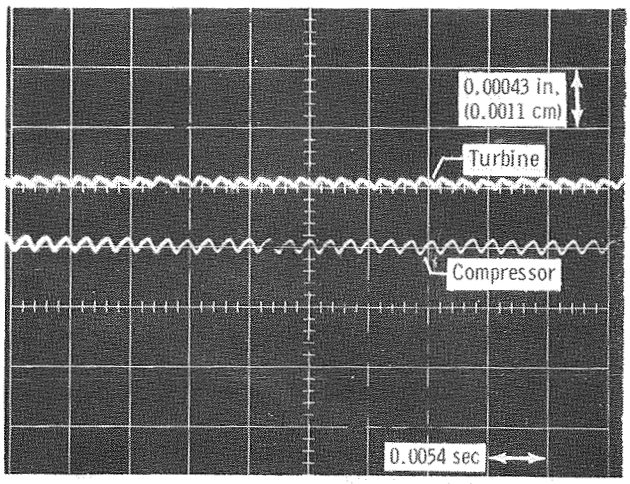

Motions of thrust runner relative to thrust stators on turbine and compressor sides of thrust bearing

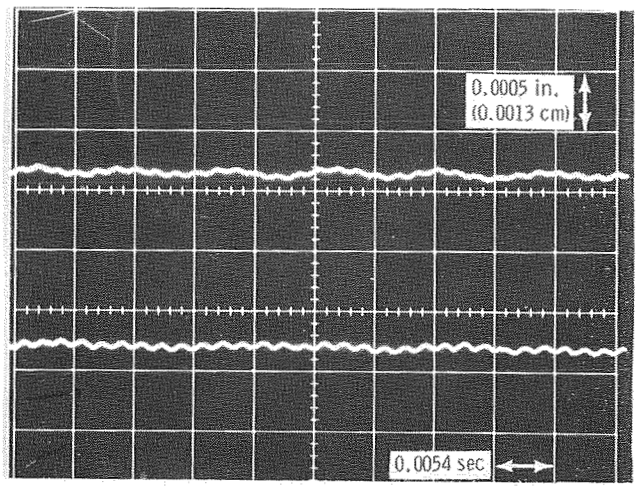

Motions of thrust stator with respect to frame; gimbal traces

(a) Turbine inlet pressure, 25.8 psia (17.8 N/cm^2 abs); turbine inlet temperature, 2060° R (1144 K).

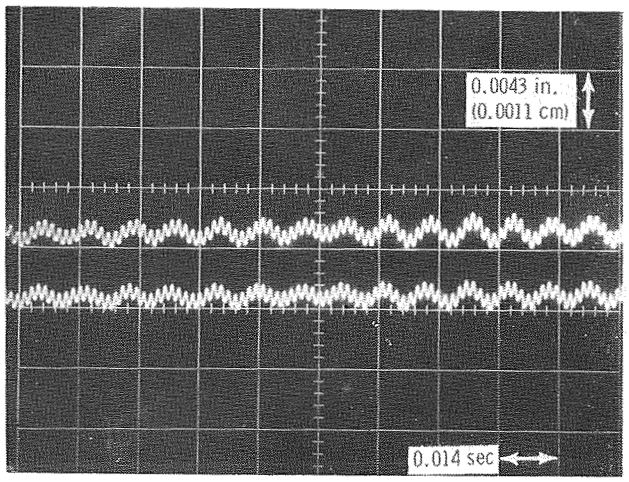

Motions of thrust runner; turbine side of bearing

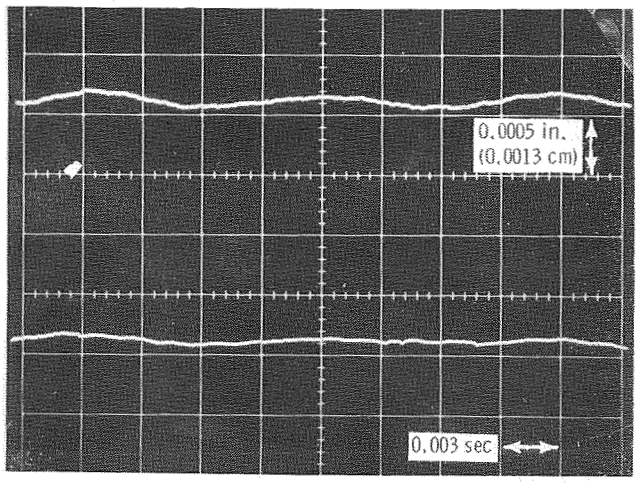

Gimbal traces

(b) Turbine inlet pressure, 45 psia (31 N/cm^2 abs); turbine inlet temperature; 1660° R (922 K).

Figure 5. - Thrust bearing and gimbal motions.

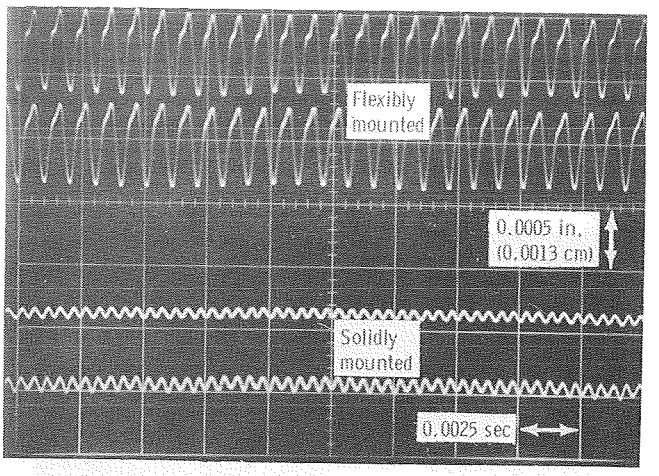

(a) Motions of leading edges of turbine journal bearing pads.

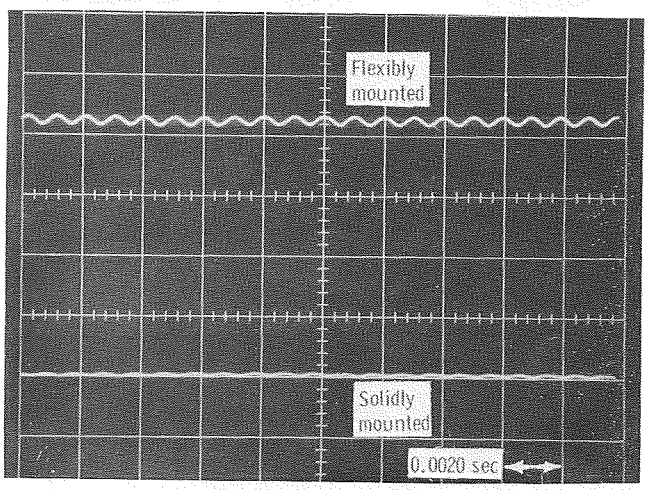

(b) Motions of leading edges of compressor journal bearing pads.

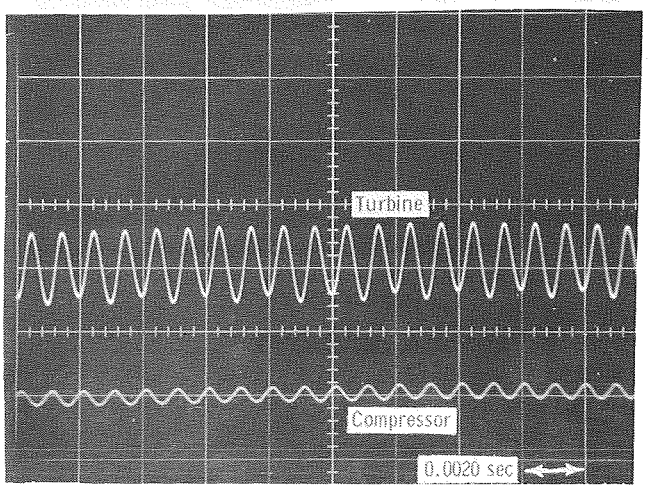

(c) Radial motions of flexibly mounted pads and pivots; turbine and compressor journal bearings.

Figure 6. - Pneumatic hammer; bearing pressure ratio, 16.2; zero speed.

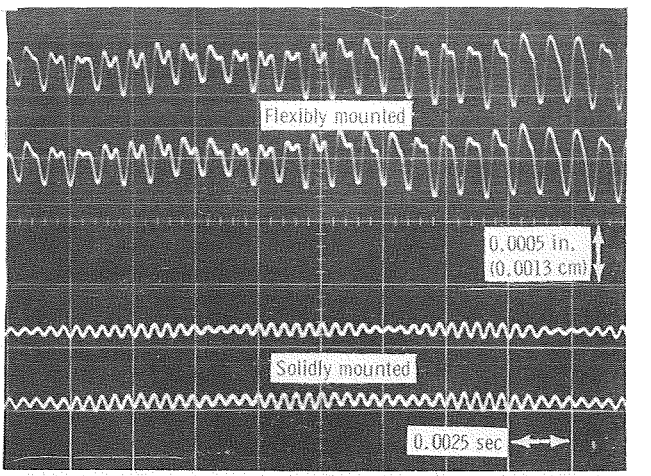

(a) Motions of leading edges of turbine journal bearing pads.

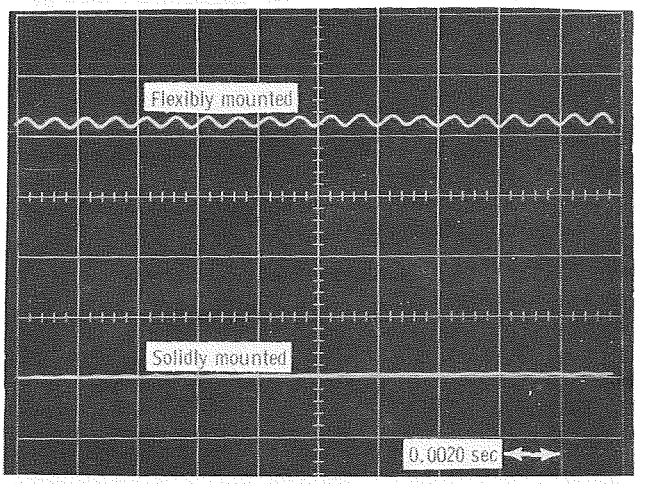

(b) Motions of leading edges of compressor journal bearing pads.

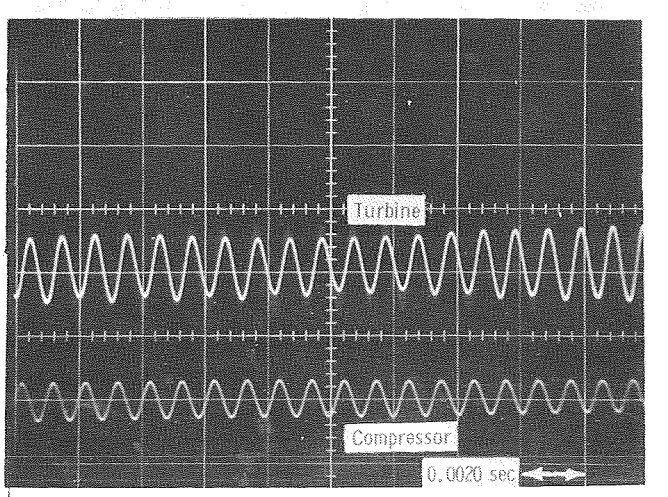

(c) Radial motions of flexibly mounted pads and pivots; turbine and compressor journal bearings.

Figure 7. - Pneumatic hammer, bearing pressure ratio, 22.4; zero speed.

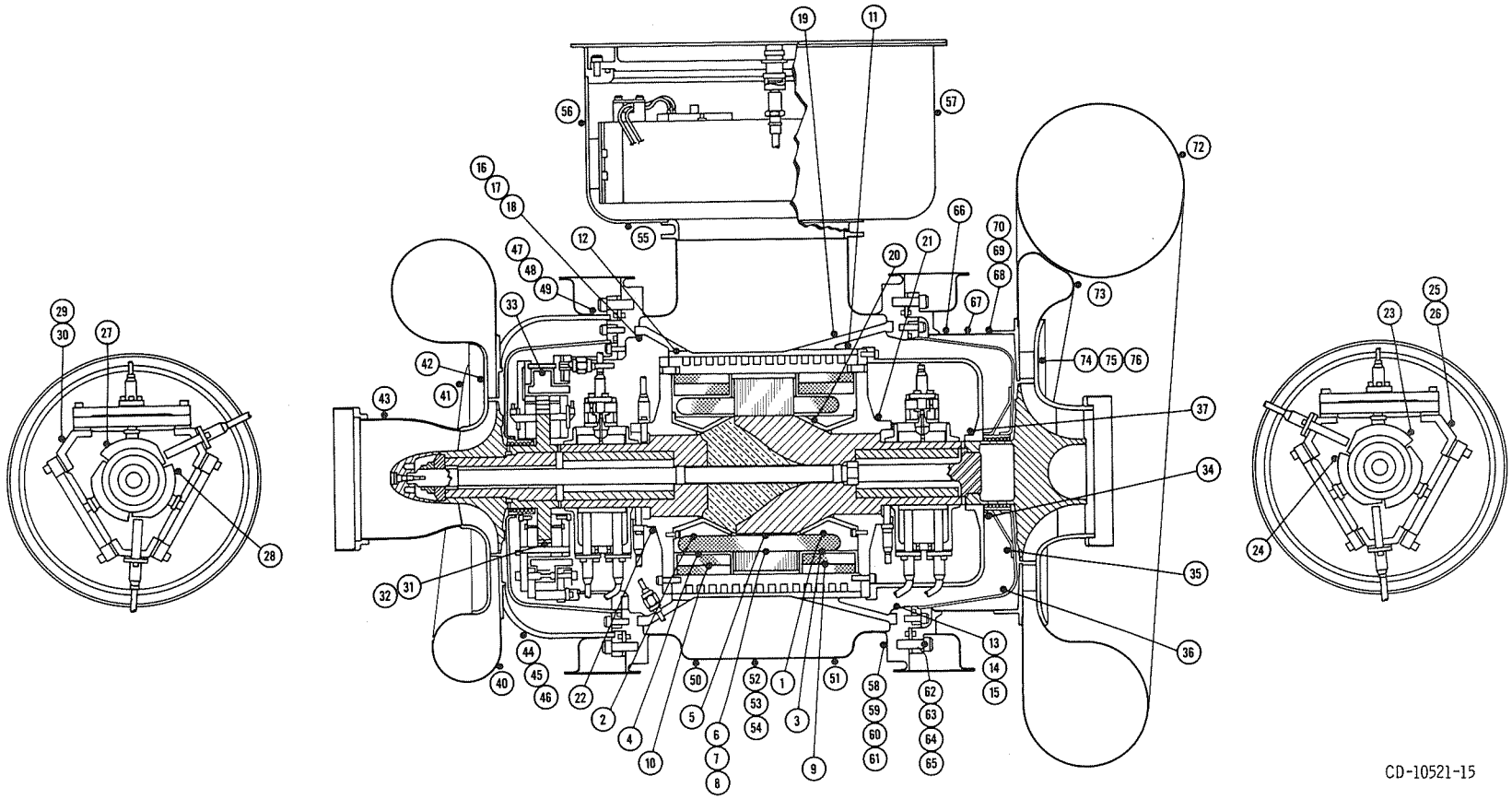

Figure 8. - Location of thermocouples in Brayton rotating unit. (Not shown are thermocouples 39, at the compressor outlet scroll, and 71, at the turbine inlet scroll.)

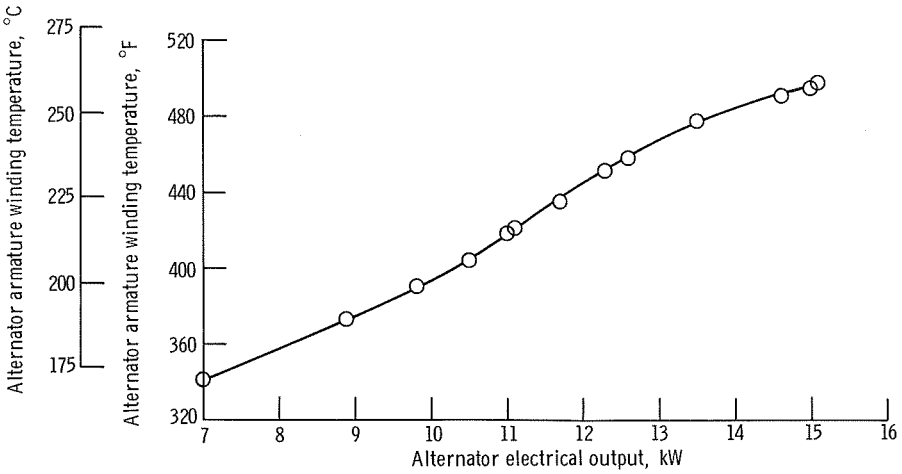

Figure 9. - Variation of alternator armature winding temperature with alternator electrical output. Turbine inlet temperature, 2060° R (1144 K).

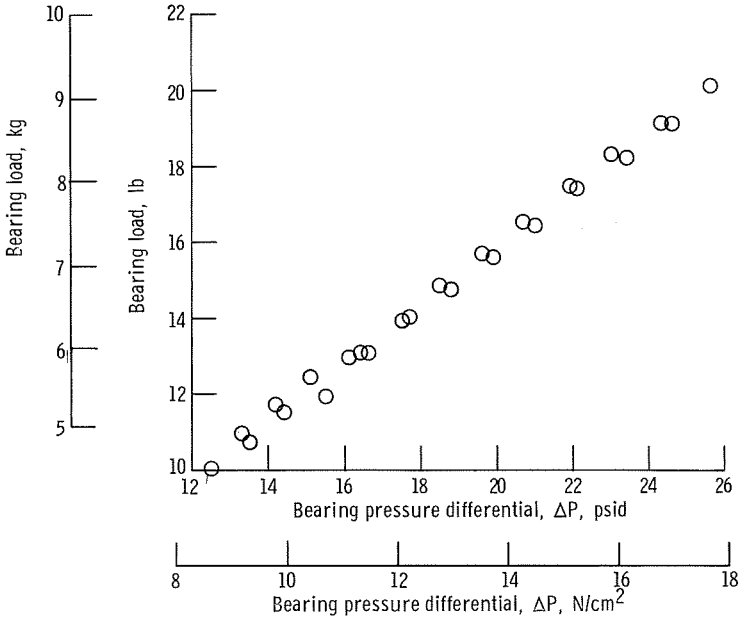

Figure 10. - Variation of bearing load with bearing pressure difference. Ambient pressure, 16 psia (11 N/cm^2 abs); speed, 36 000 rpm.

NASA-Langley, 1970 — 3 E-5456

NATIONAL AERONAUTICS AND SPACE ADMINISTRATION
WASHINGTON, D. C. 20546

OFFICIAL BUSINESS

FIRST CLASS MAIL

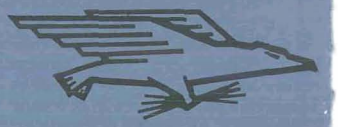

POSTAGE AND FEES PAID
NATIONAL AERONAUTICS AND
SPACE ADMINISTRATION

POSTMASTER: If Undeliverable (Section 158 Postal Manual) Do Not Return

"The aeronautical and space activities of the United States shall be conducted so as to contribute . . . to the expansion of human knowledge of phenomena in the atmosphere and space. The Administration shall provide for the widest practicable and appropriate dissemination of information concerning its activities and the results thereof."

—NATIONAL AERONAUTICS AND SPACE ACT OF 1958

NASA SCIENTIFIC AND TECHNICAL PUBLICATIONS

TECHNICAL REPORTS: Scientific and technical information considered important, complete, and a lasting contribution to existing knowledge.

TECHNICAL NOTES: Information less broad in scope but nevertheless of importance as a contribution to existing knowledge.

TECHNICAL MEMORANDUMS: Information receiving limited distribution because of preliminary data, security classification, or other reasons.

CONTRACTOR REPORTS: Scientific and technical information generated under a NASA contract or grant and considered an important contribution to existing knowledge.

TECHNICAL TRANSLATIONS: Information published in a foreign language considered to merit NASA distribution in English.

SPECIAL PUBLICATIONS: Information derived from or of value to NASA activities. Publications include conference proceedings, monographs, data compilations, handbooks, sourcebooks, and special bibliographies.

TECHNOLOGY UTILIZATION PUBLICATIONS: Information on technology used by NASA that may be of particular interest in commercial and other non-aerospace applications. Publications include Tech Briefs, Technology Utilization Reports and Notes, and Technology Surveys.

Details on the availability of these publications may be obtained from:

SCIENTIFIC AND TECHNICAL INFORMATION DIVISION
NATIONAL AERONAUTICS AND SPACE ADMINISTRATION
Washington, D.C. 20546